The Surface Chemistry of Au Colloids and Their Interactions with Functional Amino Acids

Ziyi Zhong,*,† Sergiy Patskovskyy,‡ Pierre Bouvrette,† John H. T. Luong,† and Aharon Gedanken*,§

Biotechnology Research Institute, National Research Council Canada, Montreal, Quebec, Canada H4P 2R2, Départment de Génie Physique, Ecole Polytechnique de Montréal, Case, Postale 6079, succ. Centre-ville, Montréal, Quebec, Canada, H3C 3A7, and Department of Chemistry, Bar-Ilan University, Ramat-Gan 52900, Israel

Received: October 10, 2003

The work reported here describes interactions between nanoscale Au colloids and two main types of organic functional groups, viz., alkanethiols and amino acids. The surface chemistry of particulate Au is dominated by electrodynamic factors related to its (negative) surface charge. Generalized multiparticle Mie calculations were used to model the optical absorption characteristics of Au particles, existing either singly or in varying degrees of aggregation. Experiments with standard (monodisperse) Au colloids confirm the theoretical prediction of a new peak appearing at longer wavelength that intensifies and shifts further from the original peak with increasing particle size, increasing aggregate size, or shorter interparticle spacing. Control of aggregation degree in alkanethiols is achieved by judicious selection of terminal group composition (single- or double-ended), alkyl chain length, and the presence of pH sensitive groups such as carboxylates. In amino acids, the reactivity of the α-amine (adjacent to −COOH) is found to be pH-dependent. Linking via the α-amine is activated at low pH but suppressed at intermediate and high pH due to electrostatic repulsive forces between the Au surface and the charged carboxylate group or even the (formally neutral) polar carbonyl group in amides. However, dibasic amino acids can still be used to cross-link Au colloids at high pH. The pH insensitive (remote) amine binds amino acids to each particle, leaving protruding pairs of α-amines that can be bridged by a symmetrical linker molecule like glutaraldehyde (via its electrophilic centers). This offers a new way to organize Au nanoparticles into extended architectures and functional materials over a wide range of pH. The potential of Au colloids to recognize and determine dibasic amino acids based on optical absorption changes is briefly assessed. A higher detection limit for cysteine (1.2 μg/mL) was found for larger (40 nm) Au particles.

Introduction

With their excellent compatibility with biomolecules[1−4] and distance-dependent optical absorbance,[1,5] colloidal Au nanoparticles have drawn intense scientific and technological interest. In colloidal solutions, the color of Au nanoparticles may range from red to purple, to blue and almost black, due to the formation of aggregates. This is attributable to electric dipole−dipole interactions and coupling between plasmons of neighboring particles in the aggregates.[6−8] Exploitation of this unusual phenomenon has given rise to new analytical and sensing techniques. These include, inter alia, the development of surface-enhanced Raman scattering substrates based on self-assembled Au colloid monolayers that can adsorb molecules in close space,[9,10] selective scanometric DNA detection,[11] colorimetric detection of polynucleotides[5,12] or protein interactions,[13] and colloidal Au-enhanced surface plasmon resonance immunosensing effects.[14,15]

Au colloids bearing surface negative charge are seen to readily bind thiol, amine, cyanide, or diphenylphosphine functional groups.[9,16−19] Unfortunately, the physical chemistry underpinning these interactions and the degree of influence of environmental factors remain somewhat obscure and controversial. For example, even in a newly published paper,[20] the authors claim that one type of amine group in lysine can readily bind with Au colloids, whereas the other cannot. An added complication is that surface charge adjustment via, e.g., pH change, risks aggregation of Au colloids due to loss of charge-based repulsive forces.

In this report, the surface chemistry of Au colloids was studied and several approaches to the control of the surface chemistry were proposed and exploited, including the adjustment of surface charge via exposure to mixtures of alkanethiols together with pH control. We are able to show that in amino acids, the amine group [denoted NH_2 (I)] adjacent (α) to the carboxylic acid moiety (COOH) can bind with Au nanoparticles only at relatively low pH, while there is no such kind of restriction on the more distant analogous amine [NH_2 (II)]. Thus, the connection between Au particles via amino acids, in the absence/presence of glutaraldehyde as a molecular "bridge", was achieved over a wide range of pH values. This novel type of binding is distinct from traditional linkages provided by, e.g., thiol molecules, polymer molecules,[21] or the complicated streptavidin/biotin and oligonucleotide (DNA) strand cross-linkages.[2,13,22] Experimental evidence supports the theoretical prediction that in the detection of amino acids, larger Au nanoparticles give rise to higher (photometric) signal response.

* To whom correspondence should be addressed. E-mail: Gedanken@mail.biu.ac.il. Present address: Institute of Chemical and Engineering Sciences, Block 28, Unit No. 02-08, Ayer Rajah Crescent, Singapore 139959. Fax: (65)6873-4805.

† National Research Council Canada.

‡ Ecole Polytechnique de Montréal.

§ Bar-Ilan University.

10.1021/jp037056a CCC: $27.50
Published on Web 03/05/2004

Experimental Section

Reagents and Materials. The following chemicals were obtained from Sigma and used as received: L-lysine (Lys), L-methionine (Met), DL-phenylalanine (Phe), L-aspartic acid (Asp), L-alanine (Ala), glutamine (Gln), arginine (Arg), glutamic acid (Glu), Lys α-oxidase, and gold colloids with diameters of 5, 10, and 20 nm. Hydrogen tetrachloroaurate(III) trihydrate, anhydrous ethanol, glutaraldehyde (grade II, 25% aqueous solution), and all alkanethiols (1,2-ethanedithiol, 1,3-propanedithiol, 1,4-butanedithiol, 1,5-pentanedithiol, 1,6-hexanedithiol, 1,8-octanedithiol, 1,9-nonanedithiol, 1-propane-thiol, 1-hexanethiol, 1-octanethiol, 1-nonanethiol, 11-undecanethiol, 2-mercaptoethanol, 6-mercapto-1-hexanol, 11-mercapto-1-undecanol, 3-mercaptopropionic acid, 11-mercaptoundecanoic acid, and 1,2-benzenedithiol) were purchased. Urea and ethylenediamine were purchased from Aldrich, while glycine was obtained from Bio-Rad Laboratories (CA). Filters (0.22 μm) were supplied from Corning (NY). Ultrapure deionized water was obtained from an 18 MΩ Barnstead Nanopure water filtration/purification system.

Au Colloid Preparation. Colloidal Au with average diameters of 15 and 40 nm was prepared following the literature procedures.[1,13,15] Glassware was thoroughly cleaned prior to use with freshly prepared aqua regia ($HCl:HNO_3 = 3:1$), rinsed with deionized and ultrahigh purity H_2O sequentially, and oven-dried at 100−110 °C for 2−3 h. For the preparation of 15 nm Au colloid, a 250 mL solution (1 mM) of $HAuClO_4$ in a round bottom flask was brought to the boil with vigorous stirring, and 25 mL of sodium citrate solution (38.8 mM) was rapidly added to the vortex of the solution. The solution was maintained at the boiling point with continuous stirring for about 10 min and underwent a series of color changes before finally turning red. The suspension was filtered using a 0.22 μm filter and stored at 4 °C until needed. The maximum optical absorbance was found at $\lambda_{max} \approx 520$ nm. For the 40 nm Au colloid preparation, only 2.5 mL of sodium citrate was added into the same amount of Au-containing solution. The absorbance maximum developed for this solution was at $\lambda_{max} \approx 527$ nm. The average diameters of the two Au colloid suspensions were verified by transmission electron microscopy (TEM).

Instrumental Methods and Characterization. The thiol solutions (0.01 M) were prepared in anhydrous ethanol. Usually, 1.0 mL of Au colloid solution was diluted with 1.5 mL of deionized water, and then, 100 μL of thiol solution was added. The UV−visible spectra (recorded on a DU-640 Beckman Spectrophotometer) of any Au particle/amino acid interactions were measured 20 s after mixing, unless otherwise specified. The amino acids were dissolved in buffer solutions at various pH values (The pH values in this report refer to the buffered amino acid solutions, i.e., those prior to mixing with the Au sols.) (for pH 2, 0.01 M HCl solution was used, and pH ranges 3−5 and 6−8 were obtained with 20 mM acetate and phosphate buffers, respectively). TEM measurements were conducted on a Philips CM30 TEM instrument. For TEM sample preparation of Au nanoparticles after reaction with cysteine (Cys), 5 μL of solution was dropped onto Cu grids 1 min after mixing. Excess solution on the grid was removed after 2 min with absorbent paper.

Calculation of UV−visible Spectra. Mie theory has traditionally been developed for the calculation of extinction spectra of single particles of highly symmetric shape and appropriate size range. However, in reality, a suspension of particles often has an aggregate structure of complex morphology. The complexity of the resulting multiparticle scattering and interference effects cannot be readily modeled by simple Mie theory. The discrete dipole approximation method, developed by Purcell and Pennypacker[23] and later improved by Draine,[24] is a powerful technique for modeling a suspension of irregular heterogeneous particles with mean diameters up to several times as large as the incident wavelength. Furthermore, the "T-matrix" (transition matrix), as originally proposed by Barber and Yeh[25] and developed later by Mishchenko et al.,[26] is able to treat asymmetric particles. Recently, an alternative form of T-matrix formulation, known as the generalized multiparticle Mie (GMM) solution, was developed by Xu et al.[27,28] In the GMM method, the external plane-wave incident on one particle is superimposed by the near-field Mie scattering fields of all neighboring clusters. The GMM method is very suitable for the calculation of light scattering by a cluster of spheres. Detailed information can be obtained from the Internet.[29] In our calculation, the absorption cross-section of an aggregate of gold nanoparticles was calculated for a range of wavelengths (as compared to a single wavelength in Xu's program), and a dispersion relation for Au was generated by fitting the real and imaginary parts of the index of refraction data obtained by Johnson and Christy[30] or from Innes and Sambles.[31]

Results and Discussion

1. Theoretical Calculation. Theoretical calculations reveal that the distance between Au nanoparticles, either as discrete particles or as aggregates of varying size, has a significant influence on predicted extinction spectra. Figure 1A depicts the calculated absorbance spectra (arbitrary units) for clusters of two spherical Au nanoparticles ($d = 20$ nm) with different separation distances. Highly dispersed Au nanoparticles (effectively considered as single particles) in solution should exhibit only a single peak (Figure 1A, dotted line), while linked Au particle pairs (or larger aggregates) show two absorbance maxima. The first peak, located near the resonance peak for single particles, is attributed to quadrupole plasmon excitation in coupled spheres, while the second peak at a longer wavelength is attributed to the dipole plasmon resonance of the gold nanoparticles.[32] As the interparticle spacing decreases, the first peak becomes weaker while the second peak intensifies and shifts to longer wavelengths. The maximum peak shift is observed if the interparticle distance approaches zero, at which point the electrodynamic interaction between the nanoparticles is at a maximum. At the other extreme, when the interparticle spacing exceeds about 4× the particle radius, classical single particle Mie theory should apply. In Figure 1B, the interparticle distance is fixed at 0.5 nm for Au nanoparticle pairs, since this spacing corresponds roughly to the molecular length of Cys, a dibasic amino acid group used in our experiments (vide infra). With an increase of the particle size from 5 to 40 nm, two distinct peaks develop from a broad single feature of intermediate λ_{max}. To simulate the effect of aggregation, we used a linear chain (one-dimensional) or "line cluster" model. In reality, aggregates of different shape and size are likely to be present in the solution, but as a first approximation, their tendency to aggregate and their scattering characteristics can be simulated and calculated using this model. Figure 1C shows calculated absorption spectra for line aggregates of Au nanoparticles ($d =$ 40 nm), where the light polarization direction is oriented parallel. A systematic bathochromic shift in λ_{max} is expected with increasing aggregate size. Although the dielectric constant of the surrounding medium also has an influence on the optical properties of Au nanoparticles, the effect is less pronounced than the parameters illustrated above, according to the modified

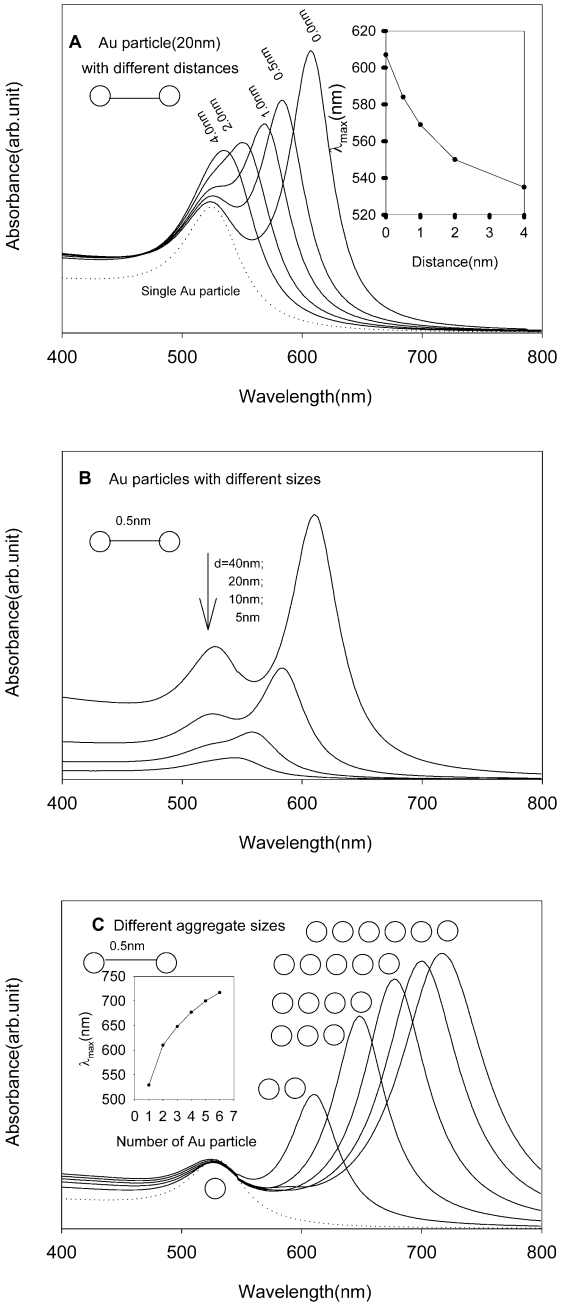

Figure 1. Electrodynamic modeling calculations for Au nanoparticles. (A) Change of extinction spectra for 20 nm diameter particles with interparticle distance (*s*). Inset is the peak shift vs interparticle distance. (B) Influence of Au nanoparticle diameter (*d*) on the extinction spectra at fixed (0.5 nm) interparticle diameter. (C) Extinction spectra of "line aggregates" of varying number ($d = 40$ nm, $s = 0.5$ nm). Inset is the peak shift against the number of Au particles in the line aggregate.

Mie theory-based calculations used here.[1,33] This reveals the trend that large Au (single) particles and/or aggregates, and short separation (or short linker molecules) between particles, should give rise to higher optical response (molar extinction). Because of the idealized model utilized here, it should be noted that the value of such calculations is restricted to prediction of qualitative trends. For more rigorous (quantitative) modeling, various additional physical phenomena must be taken into account, including electrodynamic and material effects such as electrical charging and tunneling, etc.[34]

2. Interaction of Au Colloidal Particles with Alkanethiols. The interaction of thiols with Au colloidal nanoparticles (15 nm) was extensively investigated. Figure 2 presents UV−visible spectra for Au colloidal particles associated with two different types of thiols; monothiol (with a single terminal −SH group) and dithiol (with two terminal −SH groups). For Au nanoparticles modified with monothiol molecules, micelle structures should be formed due to the hydrophobic nature of the other terminal (methyl) group projecting out from the gold particle surface.[1,9] In contrast, Au particles modified with dithiol molecules are expected to form interlinked (superlattice) structures.[2,19]

The maximum absorbance for the virgin Au sol ($d = 15$ nm) is at 520 nm (Figure 2, dotted line). With the addition of the short chain monothiol, there is a distinct and immediate bathochromic shift in λ_{max} to around 700 nm, extending beyond this wavelength after standing for 16 h (Figure 2A). In line with theoretical prediction, the shift is systematically lower with increasing length of the thiol carbon chain (Figure 2B,C). From the foregoing analysis, the observed shift is attributed mainly to the change of interspacing between Au particles. The higher background in the curves after 1-octane thiol addition (Figure 2C) is attributed to the poor aqueous solubility of this longer thiol molecule. It probably leads to the formation of flocculates, giving rise to increased light scattering. In fact, there are several processes likely to coexist as follows: (I) the diffusion of thiol molecules to the Au particles, (II) surface displacement of adsorbed anions[1,35] by thiol, (III) aggregation of modified Au particles, and (IV) precipitation of the aggregates. For monothiols with short carbon chains (Figure 2A), the color changes very fast, probably because these short molecules are less hydrophobic and react more readily with Au particles. For medium-sized monothiols (Figure 2B), the absorbance drops within several minutes after thiol addition, indicating that all four processes are rapid, including precipitation. Visual inspection confirmed the development of turbidity in the solution. At an even higher chain length (Figure 2C), only a minor change in absorbance is noted. Presumably, diffusion of the thiol (step I) becomes rate-limiting due to a lower solubility and more dilute solution.

For dithiols, the short chain variant exhibited the absorbance shift seen for the monothiol analogue but much more slowly (Figure 2D). In contrast, the longer chain variant caused rapid (blue) color development but equally rapid weakening of absorbance, suggestive of contemporaneous precipitation (Figure 2E and Figure 3A). For thiols with carboxyl (COOH) and −SH terminal groups, a peak shift could not be observed even after several months at unusually strong (0.01 M) thiol concentration (not shown).

These features can be interpreted in relation to the surface charge dynamics of the Au nanoparticles. The formation of Au aggregates from discrete particles capped with dithiol molecules will proceed faster for uncharged particles as against particles bearing residual negative charge, as would be the case for a partially (thiol-) substituted particle. However, because the interconnection between Au nanoparticles mediated by the short chain dithiol requires closer approach of two neighboring Au particles, the greater repulsive interaction would be expected to impede the process, as is observed. For thiol molecules with a carboxyl terminal group, the Au particle surface will still bear protruding negatively charged ($-COO^-$) groups after adsorption due to deprotonation (final solution pH $\approx$ 5.0), which will likewise impede close approach of Au particles, a necessary prerequisite for cross-linking (and aggregation) to proceed.

3. Control of the Surface Chemistry of Au Nanoparticles. The dominance of the surface charge effect in Au nanoparticulate systems, and how it can be utilized to advantage, is

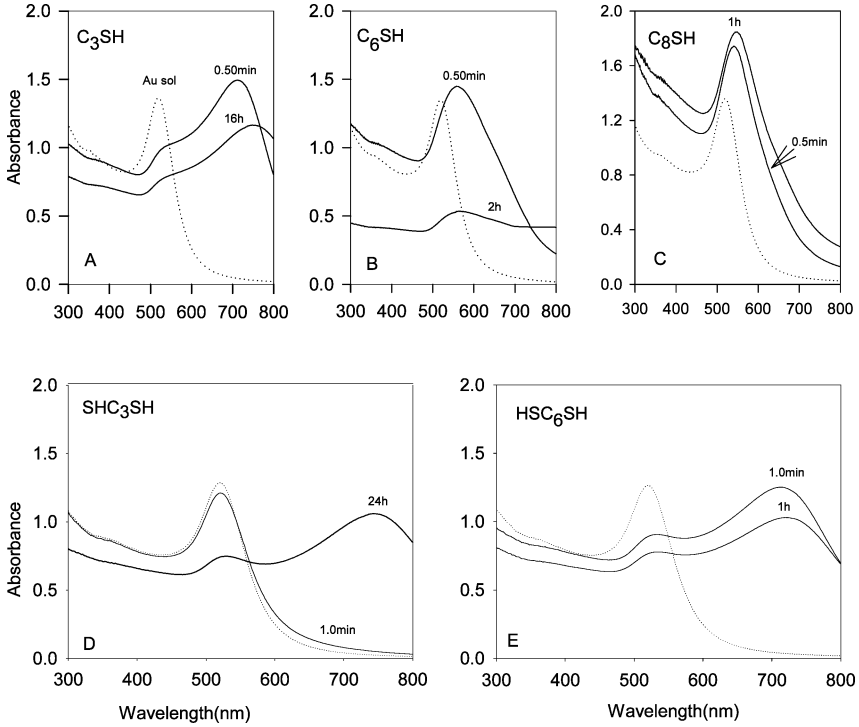

Figure 2. UV−visible spectra for Au colloidal particles (d = 15 nm) with representative mono- and bifunctional thiols. (A) 1-Propanethiol; (B) 1-hexanethiol; (C) 1-octanethiol; (D) 1,2-ethanedithiol; and (E) 1,6-hexane-dithiol. For each system, 1.0 mL of Au colloidal solution was diluted with 1.5 mL of high purity water, 100 μL of 0.01 M thiol solution in ethanol was added, and absorbance spectra were recorded at various time intervals. The control absorbance of the pure Au sol (dotted line) is plotted alongside for reference purposes.

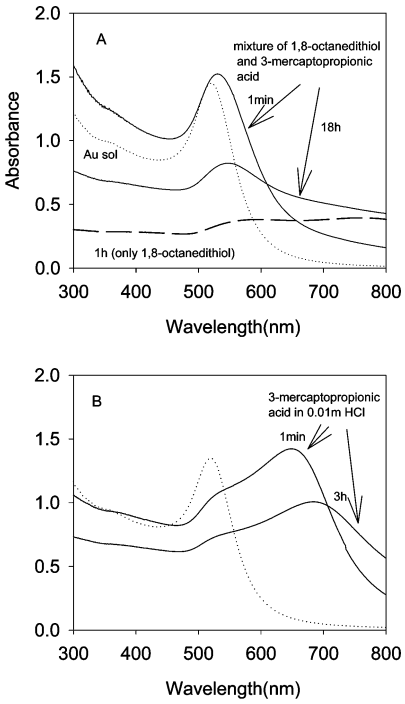

Figure 3. UV−visible spectral development and stability in colloidal gold solution with (A) a mixture of alkanethiols, 1,8-octanedithiol, and 3-mercaptopropionic acid and (B) 3-mercaptopropanoic acid at low pH (= 2).

described below (Figure 3A). 3-Mercaptopropionic acid was added to the 1,8-octanedithiol system already explored (see Figure 2E). The negatively charged carboxylate groups on the acid suppress dramatically the aggregation/precipitation process, as shown by the maintenance of a significant absorbance even after 18 h as compared to the dramatic weakening of absorbance (in its absence) after just 1 h. This example illustrates a simple but effective approach to tuning the surface reactivity of Au colloids.

The effect of pH control is shown for the same system in Figure 3B. After addition of 100 μL of 0.01 M 3-mercaptopropanonic acid solution (in 0.01 M HCl) to 1.0 mL of Au solution, a clear and rapid bathochromic shift is observed, diagnostic of aggregation. This confirms that the suppressing effect on aggregation previously seen is indeed linked to deprotonation of the carboxylate group, which does not occur here at pH 2.

4. Recognition of Amino Acids at Different pH Values: Building Novel Architectures from Au Colloids. Amino acids are constituents of proteins, and their amine (NH_2) groups are known to bind with Au particles. The influence of pH on the reaction between Au and amino acids is investigated here. As a preliminary control experiment, Figure 4A shows the optical spectra of Au colloid (1.0 mL) with sequential additions (100 μL aliquots) of 0.01 M HCl solution. There is almost no shift in the maximum peak position until the pH value is below 2.6, indicating no aggregation effects. Figure 4B shows the corresponding spectra after addition of various amino acids dissolved in 0.01 M HCl. New absorbance peaks at higher wavelength (with obvious color change) are seen for histidine (His), Cys, Lys, Arg, Met, and tyrosine (Tyr). In stark contrast, addition of Ala, Gln, Glu, or Asp produced little or no change. The primary difference in structure (excepting Tyr) is that the first group comprises those amino acids possessing two amine groups (or two similar functional groups, e.g., imidazole and thiol) in their carbon chain, whereas the second group possesses only one. It seems intuitively obvious that only dibasic amino acids can act as cross-linking agents for pairs of Au particles, thereby inducing a color change, as is observed. By the same token, at intermediate pH, dissociation of the carboxyl group[36] would be expected to hinder the binding of Au colloids via the α-amine group (I),

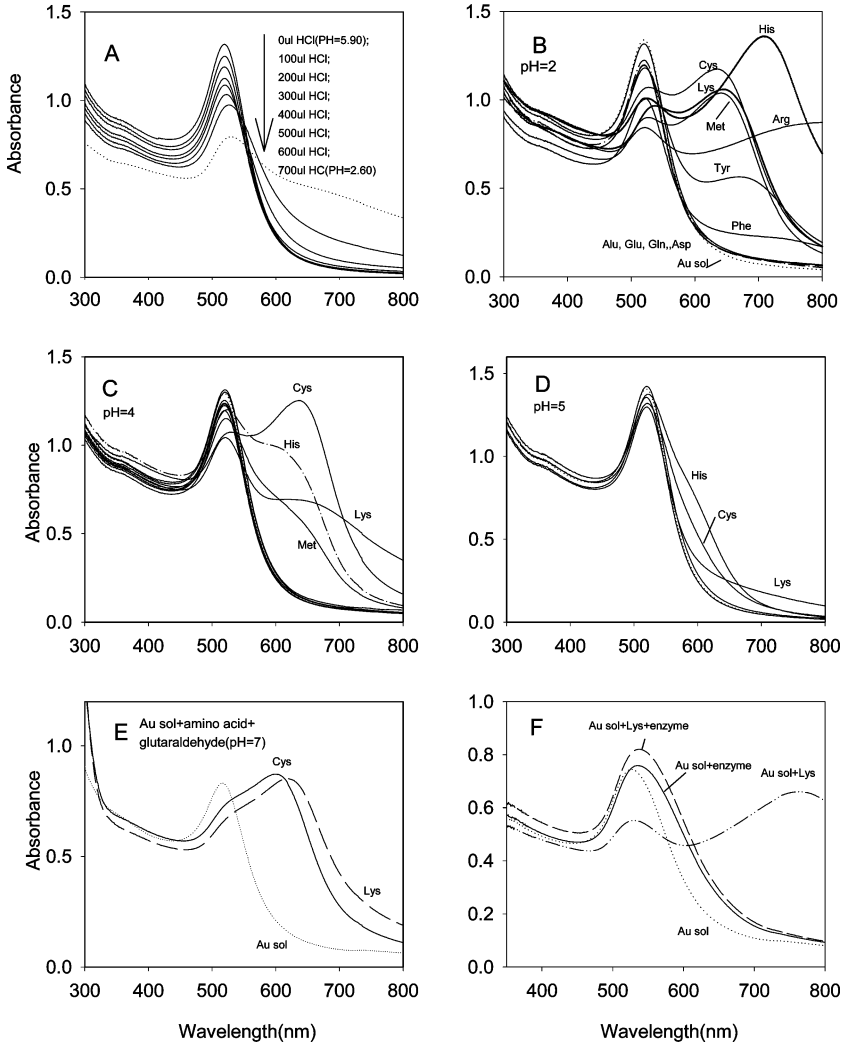

Figure 4. UV−visible spectra for Au colloidal solution with (A) 0.01 M HCl added progressively as blank effect of pH; various amino acids (100 μL, 0.01 M) at pH 2 (B), pH 4 (C), and pH 5 (D), respectively; (E) spectra after Cys or Lys addition to Au sol (pH 7) in the presence of glutaraldehyde (40 μL, 25 wt %); and (F) spectrum after reaction with treated lysine (predecarboxylated with Lys α-oxidase). For comparison, control spectra in the presence of untreated Lys and enzyme only are shown.

resulting in little or no cross-linking. Figure 4C,D shows the optical spectra at pH 4 and pH 5, respectively, for the amino acid solutions (acetate-buffered). There is clearly a progressive suppression of new color development with increasing pH, although there are interesting differences in the relative response of the different amino acids. At pH 7 (in phosphate buffer), no spectral changes whatsoever were observed for any amino acids. In contrast, inclusion of glutaraldehyde at the same pH establishes an alternate mode of cross-linking, as demonstrated in Figure 4E for Cys and Lys. This is indirect evidence that the second (remote) amine group (II) binds with Au colloids over a wide range of pH. Further evidence for this conclusion comes from reaction of Au colloids with ethylenediamine and 2-aminoethanethiol (see Supporting Information). As shown in Figure 4F, selective removal of the α-amine group (I) from Lys by treatment with Lys α-oxidase[37] eliminates normal color development (ref Figure 4B), thus confirming its involvement in binding to Au particles in a certain (low) pH range. These findings are summarized and represented in Scheme 1.

TEM images (see Figure 5A,B) verify that Au nanoparticles indeed undergo coalescence after reaction with Cys solution at pH 2. The associated color development serves to distinguish most bifunctional amino acids from their monofunctional neighbors. The new kind of linkage provided by amino acids (with glutaraldehyde acting as molecular bridge at high pH) is different from traditional linkages with dithiols or polymers.[21]

SCHEME 1: Interaction of Amine Groups with Au Colloids at Various pH Values[a]

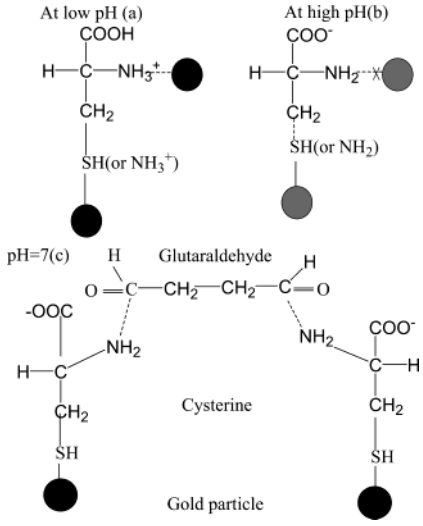

[a] Particles colored black are cross-linked; those colored gray are not.

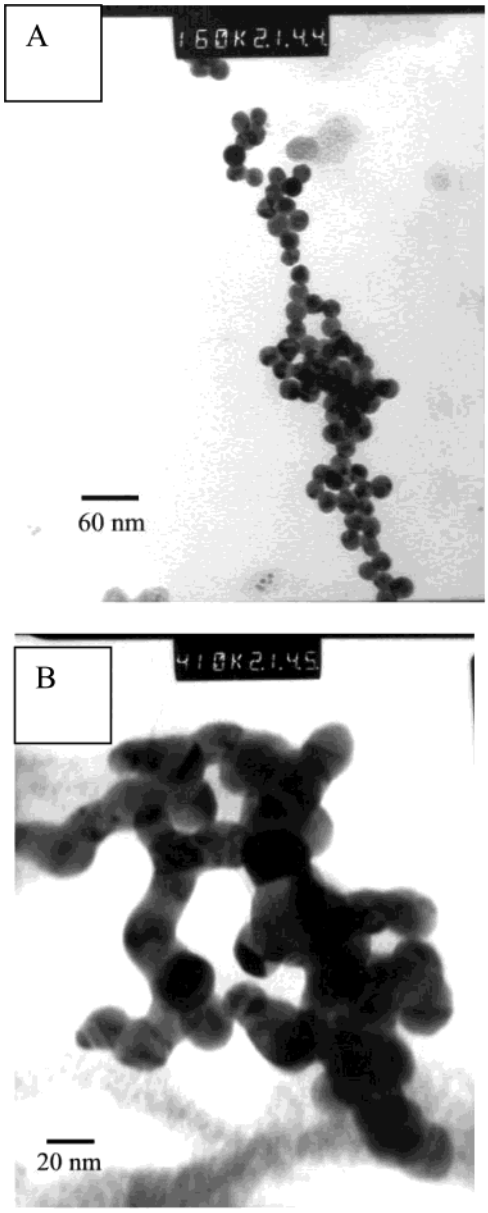

Figure 5. (A) Typical TEM image for Au nanoparticles (20 nm) reacted with Cys. (B) Magnified detail of panel A.

It is interesting to note that Gln, although dibasic, does not cross-link at any pH (Figure 4B). This suggests that even the formally neutral carbonyl group hinders binding via the adjacent amine group. To confirm this supposition, the behavior of Au colloids was compared in the presence of both urea (with carbonyl function) and ethylenediamine as otherwise similar dibasic molecules. For urea, no color change was observed at any pH, whereas ethylenediamine always induced color changes. This verifies that even the carbonyl group is sufficiently polarized to discourage linkage via an adjacent amine group. Tyr, possessing an α-amine group and a terminal hydroxyl group, appears to be a special case. Although monobasic in respect of amine groups, it nevertheless clearly facilitates cross-linking at low pH (see Figure 4B). As depicted in Scheme 2, H-bonding interactions between neighboring −OH groups are probably responsible.[38]

Amino acids Cys and Lys were chosen to study the effect of Au particle size on the relative optical absorbance change, as a basis for molecular recognition and analytical detection. As shown in Figure 6A, the smaller is the Au particle size, the less is the peak shift, and the lower is its relative intensity. In Figure 6B, the peak shift and the absorbance ratio of the new peak (Is) to the reference peak at 520 nm (Io) after Cys addition are plotted against the particle size. An almost linear increase in peak displacement (and Is/Io) against particle size is seen in the range of 5−20 nm, deviating slightly at 40 nm. Thus, the general conclusion for analytical purposes is that larger Au nanoparticles are more sensitive to the target (amino acid) molecules, which is consistent with the theoretical calculation (vide ultra).

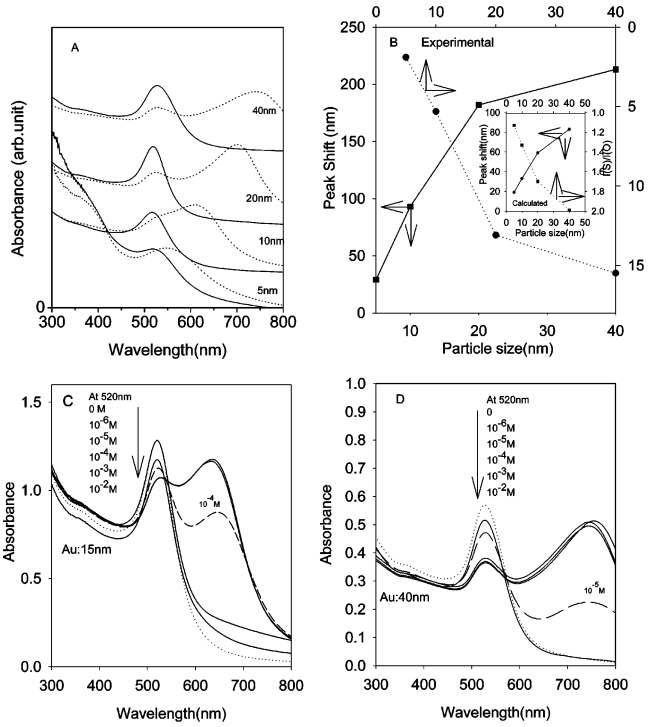

Figure 6. (A) UV−visible peak shift dependence on Au particle size, before (solid line) and after (dotted line) addition of 100 μL of 0.01 M Cys in 0.01 M HCl. (B) The ratio between the absorbance of the newly developed peak (Is) after amino acid addition to that of the "reference" peak at ∼520 nm (Io) against Au particle size (dotted line) and the corresponding peak shifts (solid line). The inset is the same plot as predicted theoretically. (C, D) Spectra of Cys at various concentrations (in 0.01 M HCl) using 15 and 40 nm diameter Au colloidal particles, respectively. The dashed curve (with concentration marked) represents the detection limit in each case.

SCHEME 2: Cross-Linking of Au Colloids via Hydrogen Bonding in Thiols Containing OH Groups

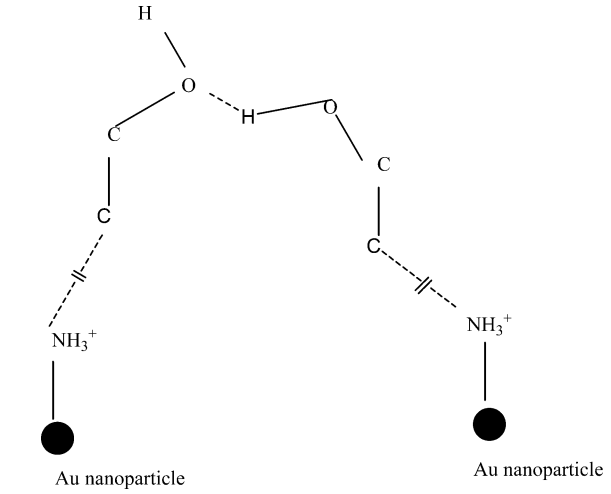

For comparison, the optical response of two different sizes of Au particles (15 and 40 nm) to a wide range of Cys concentrations is shown in Figure 6C,D, respectively. On the basis of the first appearance of a clearly-defined new peak at longer wavelength, a detection limit for Cys with 15 nm Au particles was found to be 10^{-4} M (12 μg/mL), as against 10^{-5} M (1.2 μg/mL) for 40 nm particles. A similar result was obtained for Lys (pH 2), with a detection limit of 14 μg/mL, using 15 nm Au particles.

Conclusions

In summary, the work reported here has revealed several key features of the surface chemistry of Au colloids via their adsorptive interactions with organic compounds containing various functional groups. Experiments demonstrate that the surface chemistry of colloidal Au is dominated by electrodynamic factors related to its (negative) surface charge. For alkanethiols and their carboxylic acid homologues, pH adjustment and judicious intermixing are seen to regulate or "tune" their interactions with Au nanoparticles. Likewise, in amino acids, the reactivity of the α-amine group (I, adjacent to the carboxyl group) is pH-dependent. Linking via (I) is activated at low pH but suppressed at intermediate and high pH due to electrostatic repulsive forces between the Au surface and the charged carboxylate group or even the (formally neutral) polar carbonyl group in amides. Nevertheless, cross-linking can still be facilitated in dibasic compounds at high pH using, e.g., glutaraldehyde, as a "molecular bridge" between pairs of amino acids that are in turn bound to particles via their remote, pH insensitive, amine group (II). On the basis of color development due to cross-linking of Au nanoparticles by amino acids, the photometric detection limit for Cys was found to be a sensitive function of particle size. Larger particles extend the detection limit to 10^{-5} M, in agreement with theoretical calculations using the GMM solution.

Acknowledgment. Z.Z. thanks the National Research Council Canada (NRC) for provision of a fellowship. We also thank Dr. James Highfield for his suggestions and editorial assistance.

Supporting Information Available: Spectrum of Au sol reacted with organic molecules possessing NH_2 and SH functional groups, UV−vis spectrum of Au sol with and without urea addition, and aggregates formed after Au sol reacted with Lys at low pH value. The material is available free of charge via the Internet at http://pubs.acs.org.

References and Notes

(1) Hayat, M. A. *Colloidal Gold: Principles, Methods, and Applications*; Academic Press: San Diego, CA, 1989.
(2) Mann, S.; Shenton, W.; Li, M.; Connolly, S.; Fitzmaurice, D. *Adv. Mater*. **2000**, *12*, 147−150.
(3) Mrksich, M. *Chem. Soc. Rev*. **2000**, *29*, 267−273.
(4) Bright, R. M.; Waletr, D. G.; Musick, M. D.; Jackson, M. A.; Allison, K. J.; Natan, M. J. *Langmuir* **1996**, *12*, 810−817.
(5) Elghanian, R.; Storchoff, J. J.; Mucic, R. C.; Letsinger, R. L.; Mirkin, C. A. *Science* **1997**, *277*, 1078−1081.
(6) Takeuchi, Y.; Ida, T.; Kimura, K. *Surf. Rev. Lett*. **1996**, *3*, 1205−1208.
(7) Kreibig, U.; Genzel, L. *Surf. Sci*. **1985**, *156*, 678−700.
(8) Kim, N. T.; Rosenzweig, Z. *Anal. Chem*. **2002**, *74*, 1624−1628.
(9) Freeman, R. G.; Grabar, K. C.; Allsion, K. J.; Bright, R. M.; Davis, J. A.; Guthrie, A. P.; Hommer, M. B.; Jackson, M. A.; Smith, P. C.; Walter, D. G.; Natan, M. J. *Science* **1995**, *267*, 1629−1631.
(10) Storhoff, J. J.; Mucic, R. C.; Mirkin, C. A. *J. Cluster Sci*. **1997**, *8*, 179−216.
(11) Taton, T. A.; Mirkin, C. A.; Letsinger, R. L. *Science* **2000**, *289*, 1757−1760.
(12) Storhoff, J. J.; Elghanian, R.; Mucic, R. C.; Mirkin, C. A.; Letsinger, R. L. *J. Am. Chem. Soc*. **1998**, *120*, 1959−1964.
(13) Nath, N.; Chilkoti, A. *Anal. Chem*. **2002**, *74*, 504−509.
(14) Lyon, L. A.; Musics, M. D.; Natan, M. J. *Anal. Chem*. **1998**, *70*, 5177−5183.
(15) Musick, M. D.; Keating, C. D.; Lyon, L. A.; Botsko, S. L.; Pena, D. J.; Holliway, W. D.; McEvoy, T. M.; Richardson, J. N.; Natan, M. J. *Chem. Mater*. **2000**, *12*, 2869−2881.
(16) Colvin, V. L.; Schlamp, M. C.; Alivisatos, A. P. *Nature* **1994**, *370*, 354.
(17) Grabar, K. C.; Smith, P. C.; Musick, M. D.; Davis, J. A.; Walter, D. G.; Jackson, M. A.; Guthrie, A. P.; Natan, M. J. *J. Am. Chem. Soc*. **1996**, *118*, 1148−1153.
(18) Grabar, K. C.; Allison, K. J.; Baker, B. E.; Bright, R. M.; Brown, K. R.; Freeman, R.G.; Fox, A. P.; Keating, C. D.; Musick, M. D.; Natan, M. J. *Langmuir* **1996**, *6*, 1519.
(19) Brust, M.; Bethell, D.; Schiffrin, D. J.; Kiely, C. J. *Adv. Mater*. **1995**, *7*, 795−798.
(20) Selvakannan, P. R.; Mandal, S.; Phadtare, S.; Pasricha, R.; Sastry, M. *Langmuir* **2003**, *19*, 3545.
(21) Schmitt, J.; Decher, G.; Dressick, W. J.; Brandow, S. L.; Geer, R. F.; Shashidhar, R.; Calvert, J. M. *Adv. Mater*. **1997**, *9*, 61−65.
(22) Storhoff, J. J.; Lazarides, A. A.; Mucic, R. C.; Mirkin, C. A.; Letsinger, R. L.; Schatz, G. C. *J. Am. Chem. Soc*. **2000**, *122*, 4620−2650.
(23) Puecell, E. M.; Pennypacker, C. R. *Astrophys. J*. **1973**, *186*, 705.
(24) Draine, B. T. *Astrophys. J*. **1988**, *333*, 848.
(25) Barber, P. W.; Yeh, C. *Appl. Opt*. **1975**, *14*, 2864.
(26) Mishchenko, M. I.; Travis, L. D.; Mackowski, D. W. *J. Quant. Spectrosc. Radiat. Transfer* **1996**, *55*, 535.
(27) Xu, Y. L.; Wang, R. T. *Phys. Rev. E* **1998**, *58*, 3931−3948.
(28) Xu, Y. L. *Appl. Opt*. **1997**, *36*, 9496−9508.
(29) See Internet web-site http://www.astro.ufl.edu/∼Xu.
(30) Johnson, P. B.; Christy, R. W. *Phys. Rev. B* **1972**, *6*, 4370−4379.
(31) Innes, R. A.; Sambles, J. R. *J. Phys. F* **1987**, 277−287.
(32) Jensen, T.; Lelly, L.; Lazarides, A.; Schatz, G. C. *J. Cluster Sci*. **1999**, *10*, 295−317.
(33) Schmitt. J.; Machtle. P.; Eck, D.; Mohwald, H.; Helm, C. A. *Langmuir* **1999**, *15*, 3256−3266.
(34) Kreibig, U.; Hilger, A.; Hovel, M. Quantum Optical Properties of Free and Embedded Metal Clusters: Recent Results. In *Large Clusters of Atoms and Molecules*; Martin, T. P., Ed.; Kluwer: Norwell, MA, 1996; pp 475−494.
(35) Yaminky, V.; Ninham, B. W. *Langmuir* **1996**, *13*, 4969−4970.
(36) Nerg, J. M.; Tymoczko, J. L.; Stryer, L. *Biochemistry*, 5th ed.; W. H. Freeman and Co.: New York, 2002; Chapter 3, pp 41−76.
(37) Kussakabe, H.; Kodama, K.; Kuninaka, A.; Yoshino, H.; Minoso, H.; Soda, K. *J. Biol. Chem*. **1980**, *265*, 976−981.
(38) (a) Boal, A. K.; Rotello, V. M. *Langmuir* **2000**, *16*, 9527−9532. (b) Paulini, R.; Frankamp, B. L.; Rotello, V. M. *Langmuir* **2002**, *18*, 2368−2373.